ELSEVIER

Journal of Chromatography A, 776 (1997) 3–13

JOURNAL OF CHROMATOGRAPHY A

# Model discrimination and estimation of the intraparticle mass transfer parameters for the adsorption of bovine serum albumin onto porous adsorbent particles by the use of experimental frontal analysis data

G.A. Heeter[a], A.I. Liapis[a,b,*]

[a]*Department of Chemical Engineering and Biochemical Processing Institute, University of Missouri-Rolla, Rolla, MO 65401-0249, USA*

[b]*Lehrstuhl B für Verfahrenstechnik, Technische Universität München, Arcisstrasse 21, D-80333 München, Germany*

**Abstract**

Experimental data from a chromatographic system involving the adsorption of bovine serum albumin (BSA) onto porous anion-exchange adsorbent particles packed in a column are presented. The parameters that characterize the mass transfer mechanisms of intraparticle diffusion and convection are estimated by fitting the predictions of dynamic mathematical models describing adsorption in column systems having spherical perfusive and purely diffusive adsorbent particles to the experimental breakthrough data obtained from the column adsorption system. Both linear and nonlinear expressions for the equilibrium isotherm are considered. The values of the transport parameters are estimated in the time domain for the nonlinear adsorption models and in the Laplace transform domain for the linear adsorption models. The capabilities of the different models to describe satisfactorily the dynamic behavior of the adsorption system are compared. The dynamic nonlinear adsorption model for purely diffusive particles is found to describe most appropriately the dynamic behavior of the experimental chromatographic system studied in this work. © 1997 Elsevier Science B.V.

*Keywords:* Mathematical models; Frontal analysis; Intraparticle mass transfer; Adsorption; Albumin; Proteins

## 1. Introduction

Mathematical models describing liquid adsorption in finite bath systems [1–3] and in column systems [3–13] which consider the various adsorption and mass transfer mechanisms of the adsorption process have been presented and their theoretical implications studied to provide information concerning the dynamic behavior of the adsorption systems in various operating modes and the relative importance of the adsorption and mass transfer mechanisms occurring in the adsorption systems. The parameters of these models that characterize the intraparticle mass transfer mechanisms can not presently be determined by direct measurements; they can, however, be estimated by matching the dynamic predictions of appropriate mathematical models with the dynamic experimental data from the adsorption system of interest.

If the expression for the adsorption equilibrium isotherm that is used in a particular dynamic adsorption model is nonlinear, then the solution to that

*Corresponding author.


*PII* S0021-9673(97)00439-1

model is obtained numerically. Parameter estimation using a nonlinear adsorption model will therefore involve the repeated numerical solution of the partial differential equations that make up the model, requiring significant computational resources [14].

However, analytical solutions in the Laplace transform domain have been developed for mathematical models of finite bath and column adsorption systems in which the equilibrium isotherm expression is linear [15–17]. The estimation of parameters using these linear adsorption models can be done in the Laplace transform domain [15,16]. The parameter estimation procedure in the Laplace transform domain involves the solution of algebraic equations which are significantly simpler and easier to solve than the partial differential equations of the time domain.

In this work, the results of frontal analysis experiments on a chromatographic system involving the adsorption of bovine serum albumin (BSA) onto porous anion-exchange particles are presented. These dynamic experimental data are then used to estimate the values of the parameters that characterize the intraparticle mass transfer mechanisms of the adsorption process in models with perfusive and with purely diffusive adsorbent particles. Dynamic adsorption models in which the expression for the adsorption equilibrium isotherm is linear and nonlinear are considered. The values of the parameters are estimated in the Laplace transform domain for the linear adsorption models and in the time domain for the nonlinear adsorption models. The values of the estimated parameters are used to discriminate between different models.

## 2. Theory

Adsorption is considered to take place from a flowing liquid stream in a fixed bed of spherical adsorbent particles having a monodisperse porous structure under isothermal conditions. The differential mass balance for the adsorbate in the flowing fluid stream in the column is given by

$$\frac{\partial C_d}{\partial t}+\frac{V_f}{\varepsilon}\frac{\partial C_d}{\partial x}=-\frac{(1-\varepsilon)}{\varepsilon}\frac{\partial \overline{C}_p}{\partial t} \tag{1}$$

The average adsorbate concentration in the adsorbent particle, $\overline{C}_p$, is given by Eq. (2) as follows:

$$\overline{C}_p=\frac{3}{2R_p^3}\left[\int_0^{\pi}\int_0^{R_p}\varepsilon_p C_p R^2\sin\theta\,dR\,d\theta+\int_0^{\pi}\int_0^{R_p}C_s R^2\sin\theta\,dR\,d\theta\right] \tag{2}$$

The initial and boundary conditions of Eq. (1) are

$$\text{at } t=0,\ C_d=0,\ 0\le x\le L \tag{3}$$

$$\text{at } x=0,\ C_d=C_{d,in},\ t>0 \tag{4}$$

The mechanisms of external film mass transfer around the adsorbent particles and axial dispersion in the column are considered to have negligible contribution to the overall mass transfer resistance for reasons discussed in the literature [18,19].

The differential mass balance for the adsorbate in a spherical adsorbent particle having a monodisperse porous structure in which the intraparticle mass transfer mechanisms of convection and diffusion could occur is given by

$$\frac{\partial C_p}{\partial t}+v_{pR}\frac{\partial C_p}{\partial R}+v_{p\theta}\left(\frac{1}{R}\right)\frac{\partial C_p}{\partial \theta}+\left(\frac{1}{\varepsilon_p}\right)\frac{\partial C_s}{\partial t}=D_p\left[\left(\frac{1}{R^2}\right)\frac{\partial}{\partial R}\left(R^2\frac{\partial C_p}{\partial R}\right)+\left(\frac{1}{R^2\sin\theta}\right)\frac{\partial}{\partial\theta}\left(\sin\theta\,\frac{\partial C_p}{\partial\theta}\right)\right] \tag{5}$$

The initial and boundary conditions of Eq. (5) are as follows:

$$\text{at } t=0,\ C_p=0,\ 0\le R\le R_p \tag{6}$$

$$\text{at } t=0,\ C_s=0,\ 0\le R\le R_p \tag{7}$$

$$\text{at } R=R_p,\ C_p=C_d(t,x),\ t>0,\ 0\le\theta\le\pi \tag{8}$$

$$\text{at } R=0,\ C_p \text{ is finite},\ t>0,\ 0\le\theta\le\pi \tag{9}$$

$$\text{at } \theta=0,\ \left.\frac{\partial C_p}{\partial\theta}\right|_{\theta=0}=0,\ 0\le R\le R_p \tag{10}$$

$$\text{at } \theta=\pi,\ \left.\frac{\partial C_p}{\partial\theta}\right|_{\theta=\pi}=0,\ 0\le R\le R_p \tag{11}$$

The intraparticle velocity components in Eq. (5) are

obtained from the following expressions [9,13,20,21]:

$$v_{pR} = FV_f \cos\theta \quad (12)$$

$$v_{p\theta} = -FV_f \sin\theta \quad (13)$$

The parameter $F$ in Eqs. (12) and (13), which can be considered to represent the fraction of the column fluid superficial velocity, $V_f$, that is flowing through the pores of the adsorbent particle [21], characterizes the mass transfer mechanism of intraparticle convection. When $F>0$, intraparticle fluid flow exists, and, as in previous publications [6–13], we consider any adsorbent particles in which the intraparticle velocity vector, $\mathbf{v}_p$, is non-zero to be perfusive particles. When $F=0$, the adsorbent particles are purely diffusive.

In order to solve this system of partial differential equations, an expression for the accumulation term $\partial C_s/\partial t$ in Eq. (5) is required. In this work, the interaction between the adsorbate molecules and the active sites on the surface of the pores of the adsorbent particles is taken to occur infinitely fast, and, therefore, local equilibrium between the adsorbate in the pore fluid and in the adsorbed phase at each point in the pores is considered to exist and the expression for the accumulation term $\partial C_s/\partial t$ in Eq. (5) is obtained from the equilibrium adsorption isotherm. Two models for the equilibrium adsorption isotherm are considered in this work. In the dynamic model with a linear isotherm, the expression for the equilibrium adsorption isotherm is given by

$$C_s = HC_p \quad (14)$$

The solution in the Laplace transform domain of the dynamic model with a linear equilibrium isotherm given by Eq. (14) has been presented in [16]. Also in [16], a method was presented for estimating in the Laplace transform domain the parameters that characterize the mechanisms of intraparticle diffusion and convection in spherical adsorbent particles packed in a column. In this method, the experimental breakthrough curve obtained from frontal analysis is represented by a function of time for which the Laplace transform can be obtained. The prediction of the linear adsorption model for the breakthrough curve in the Laplace transform domain is then fitted to a dataset generated in the Laplace transform domain from the function in the Laplace transform domain that represents the experimental breakthrough curve.

In the dynamic model with a nonlinear isotherm, the Langmuir equilibrium isotherm,

$$C_s = \frac{KC_T C_p}{1 + KC_p} \quad (15)$$

is used. When Eq. (15) is used for the equilibrium adsorption isotherm, the accumulation term $\partial C_s/\partial t$ in Eq. (5) is given by

$$\frac{\partial C_s}{\partial t} = \frac{KC_T}{(1 + KC_p)^2}\frac{\partial C_p}{\partial t} \quad (16)$$

Eq. (16) is substituted into Eq. (5) to obtain the dynamic adsorption model with a nonlinear equilibrium isotherm. The solution in the time domain of the dynamic adsorption model with a nonlinear equilibrium isotherm is obtained by the numerical solution procedure reported in [9,22]. The values of the parameters that characterize the mechanisms of intraparticle diffusion and convection could be estimated by fitting the dynamic prediction of the nonlinear model obtained by numerical solution in the time domain to the experimental breakthrough curve obtained from frontal analysis experiments.

## 3. Experimental

### 3.1. Materials

The bovine serum albumin was obtained from Sigma (St. Louis, MO, USA; Catalog No. A-4378). Solutions were prepared in 20 m*M* Bis-tris buffer (pH 7.0) and a solution of 1 *M* NaCl was used for elution. The Bis-tris Propane and the NaCl were also obtained from Sigma.

### 3.2. Apparatus

A Resource Q 1 ml column (Pharmacia Biotech, Uppsala, Sweden) was used. This 30 mm×6.4 mm diameter column was packed by the manufacturer with Source 15Q ion-exchange media, which consists of 15 μm diameter strong anion-exchange particles. Flow to the column was maintained by a Beckman Model 110B pump (Beckman, San Ramon,

CA, USA) and the column effluent was monitored at 280 nm by an ISCO UA-5 Absorbance/Fluorescence detector (ISCO, Lincoln, NE, USA). Data collection was with a Metrabyte PC Bus I/O Board and Control EQ software (Quinn-Curtis, Newton, MA, USA).

### 3.3. Procedure

All experiments were conducted at room temperature. The column was equilibrated by flowing buffer solution until a stable baseline was achieved. The protein solution was then introduced and the flow-rate maintained constant until the concentration of protein in the outlet stream was equal to that in the inlet stream. The column was then washed with buffer solution and the adsorbed protein was eluted with a solution of 1 *M* NaCl.

The value of the protein concentration in the column outlet stream was recorded at 2 s intervals during the adsorption phase of the cycle. These data were averaged in groups of 30 to give a dataset containing points at 1 min intervals to be used for analysis. The equilibrium value of the adsorbate concentration in the adsorbed phase, $C_s^*$, when the equilibrium value of the adsorbate concentration in the pore fluid is equal to the column inlet adsorbate concentration, $C_{d,in}$, was determined from this dataset using the following expression [23],

$$C_s^* = C_{d,in}\left(\frac{V_f}{L(1-\varepsilon)}\right)\left[t_b - \int_0^{t_b}\frac{C_{d,out}}{C_{d,in}}\,dt\right] - \left[\frac{\varepsilon}{1-\varepsilon} + \varepsilon_p\right]C_{d,in} \quad (17)$$

where $t_b$ is the time at which $C_{d,out} = C_{d,in}$.

## 4. Results and discussion

Frontal analysis experiments were conducted at five different values of the column inlet adsorbate concentration: $C_{d,in} = 0.01$, 0.02, 0.03, 0.04 and 0.05 kg/m$^3$. All other conditions were held constant and the values of the parameters that were considered fixed are listed in Table 1.

The equilibrium adsorption isotherm for BSA on Source 15Q anion-exchange particles is shown in Fig. 1. The points in Fig. 1 represent experimental values determined from the breakthrough data using Eq. (17) and the curve represents the best fit to these data using the Langmuir isotherm model (Eq. (15)). The Langmuir parameters that provided the best fit were $C_T = 50.82$ kg/m$^3$ and $K = 472.1$ m$^3$/kg. The Langmuir isotherm model with these parameter values represents very well the experimental equilibrium data for this system in the fluid phase adsorbate concentration range 0.01–0.05 kg/m$^3$.

Table 1
Values of the parameters of the experimental adsorption system that were considered fixed

| Parameter | Value |
|---|---|
| $d_p$ | $15\times10^{-6}$ m |
| $L$ | 0.03 m |
| $V_f$ | $2.021\times10^{-3}$ m/s |
| $\varepsilon$ | 0.35 |
| $\varepsilon_p$ | 0.48 |

The shape of the pore size distribution of Source 15Q anion-exchange particles [24] indicates that it could be appropriate to model these particles as having a monodisperse porous structure. The dynamic nonlinear adsorption model for purely diffu-

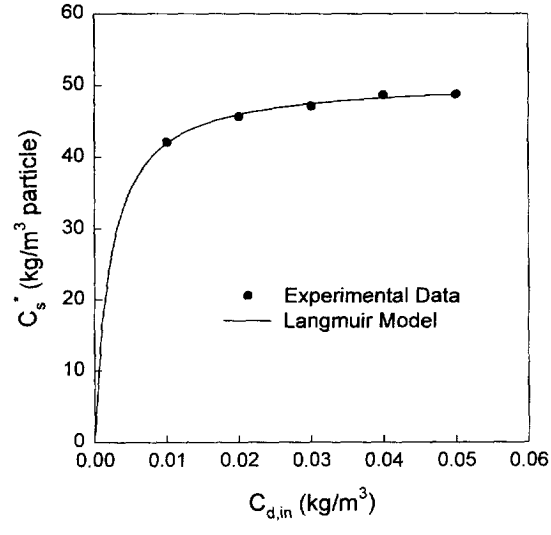


Fig. 1. Equilibrium adsorption isotherm for the adsorption of BSA onto Source 15Q anion-exchange particles. The values of the parameters of the Langmuir model are $C_T = 50.82$ kg/m$^3$ particle and $K = 472.1$ m$^3$/kg.

sive adsorbent particles with a monodisperse porous structure was fitted to the experimental breakthrough curves for $C_{d,in}=0.01$, 0.03 and 0.05 kg/m$^3$ under three conditions. For Case 1, the Langmuir isotherm parameter values that were estimated from the equilibrium experimental data ($C_T=50.82$ kg/m$^3$ and $K=472.1$ m$^3$/kg) were used and the value of $D_p$ that gave the best fit when the experimental points were evenly weighted was estimated. For Case 2, the Langmuir isotherm parameter values of $C_T=50.82$ kg/m$^3$ and $K=472.1$ m$^3$/kg were also used and the value of $D_p$ that gave the best fit when the experimental points on the lower half of the breakthrough curve (those for which $C_{d,out}/C_{d,in}\leq 0.50$) were weighted 1000 times greater than the experimental points on the upper half of the breakthrough curve, was estimated. And for Case 3, the value of the Langmuir isotherm parameter $K$ was fixed at 472.1 m$^3$/kg and the values of $D_p$ and $C_T$ that gave the best fit when the experimental points on the lower half of the breakthrough curve (those for which $C_{d,out}/C_{d,in}\leq 0.50$) were weighted 1000 times greater than the experimental points on the upper half of the breakthrough curve, were estimated. Cases 2 and 3 reflect the fact that the ability of the model to predict the breakthrough time for early breakthrough is important, since in practical applications, the adsorption process would be stopped by column switching well before $C_{d,out}/C_{d,in}=0.50$. The values of the effective pore diffusion coefficient, $D_p$, that were estimated for Cases 1–3 are presented in Table 5.

The predictions of the nonlinear model using the values of $D_p$ estimated for Case 1 are compared to the experimental breakthrough curves in Fig. 2, which shows the overall excellent agreement between the model and the experimental data. However, the dynamic nonlinear model for purely diffusive adsorbent particles with a monodisperse porous structure using the values of $D_p$ estimated for Case 1 does predict the earliest breakthrough times to be slightly later than the experimental data for $C_{d,in}=0.05$ kg/m$^3$ and $C_{d,in}=0.03$ kg/m$^3$. In Fig. 3, the predictions of the nonlinear model using the values of $D_p$ estimated for Case 2 are compared to the experimental breakthrough curves. The overall agreement between the model and the experimental data for Case 2 is not significantly different from that

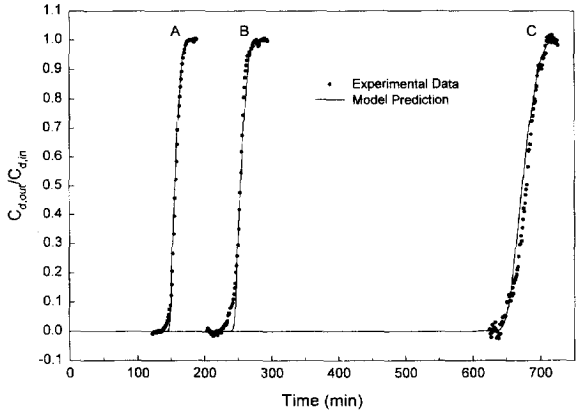


Fig. 2. Comparison of the experimental breakthrough curves with the predictions of the dynamic nonlinear adsorption model for purely diffusive adsorbent particles with a monodisperse porous structure using the best estimates of $D_p$ when the experimental points are evenly weighted. (A) $C_{d,in}=0.05$ kg/m$^3$, $D_p=2.00\times 10^{-11}$ m$^2$/s; (B) $C_{d,in}=0.03$ kg/m$^3$, $D_p=2.93\times 10^{-11}$ m$^2$/s; (C) $C_{d,in}=0.01$ kg/m$^3$, $D_p=4.11\times 10^{-11}$ m$^2$/s.

for Case 1. The comparison between the predictions of the nonlinear model using the values of $D_p$ and $C_T$ estimated for Case 3 and the experimental breakthrough curves is shown in Fig. 4. The agreement between the model and the experimental data for Case 3 is better than that for Cases 1 and 2 at early

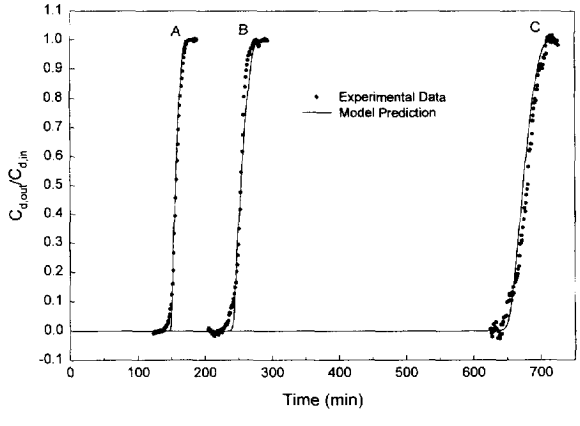


Fig. 3. Comparison of the experimental breakthrough curves with the predictions of the dynamic nonlinear adsorption model for purely diffusive adsorbent particles with a monodisperse porous structure using the best estimates of $D_p$ when the experimental points on the lower half of the breakthrough curve are more heavily weighted. (A) $C_{d,in}=0.05$ kg/m$^3$, $D_p=2.27\times 10^{-11}$ m$^2$/s; (B) $C_{d,in}=0.03$ kg/m$^3$, $D_p=2.33\times 10^{-11}$ m$^2$/s; (C) $C_{d,in}=0.01$ kg/m$^3$, $D_p=4.69\times 10^{-11}$ m$^2$/s.

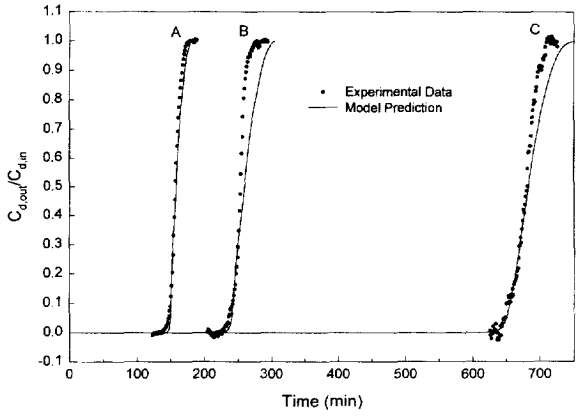


Fig. 4. Comparison of the experimental breakthrough curves with the predictions of the dynamic nonlinear adsorption model for purely diffusive adsorbent particles with a monodisperse porous structure using the best estimates of $D_p$ when the experimental points on the lower half of the breakthrough curve are more heavily weighted and $C_T$ is used as an adjustable parameter. (A) $C_{d,in}=0.05$ kg/m$^3$, $D_p=1.57\times10^{-11}$ m$^2$/s, $C_T=51.56$ kg/m$^3$ particle; (B) $C_{d,in}=0.03$ kg/m$^3$, $D_p=1.34\times10^{-11}$ m$^2$/s, $C_T=52.08$ kg/m$^3$ particle; (C) $C_{d,in}=0.01$ kg/m$^3$, $D_p=2.95\times10^{-11}$ m$^2$/s, $C_T=51.56$ kg/m$^3$ particle.

breakthrough times and much worse at later breakthrough times.

The experimental breakthrough times for 1%, 5%, 10%, 20% and 30% breakthrough (i.e., $C_{d,out}/C_{d,in}=0.01$, 0.05, 0.10, 0.20 and 0.30) are compared to the breakthrough times predicted by the dynamic nonlinear model with the estimated parameter values for Cases 1–3 for $C_{d,in}=0.01$, 0.03 and 0.05 kg/m$^3$ in Tables 2–4, respectively. In Table 2, it can be seen that there is no more than a 1% difference between the experimental breakthrough times and any of the breakthrough times predicted by the nonlinear model using the estimated parameters of Cases 1–3 for $C_{d,in}=0.01$ kg/m$^3$, up to 30% breakthrough. For $C_{d,in}=0.03$ kg/m$^3$ in Table 3, the differences between the experimental breakthrough times and the breakthrough times predicted by the nonlinear model using the estimated value of $D_p$ of Case 1 are 6.9% at 1% breakthrough and 4.2% at 5% breakthrough. Using the estimated value of $D_p$ of Case 2 slightly improves the agreement between the model and the

Table 2
Experimental and theoretical values of the breakthrough times for various values of $C_{d,out}/C_{d,in}$ when $C_{d,in}=0.01$ kg/m$^3$

| $C_{d,out}/C_{d,in}$ | Breakthrough time (min) | | | | | | |
|---|---|---|---|---|---|---|---|
| | Experimental value | Case 1 | | Case 2 | | Case 3 | |
| | | Theoretical value | % diff. | Theoretical value | % diff. | Theoretical value | % diff. |
| 0.01 | 640.4 | 642.4 | +0.3 | 646.1 | +0.9 | 638.0 | −0.3 |
| 0.05 | 647.6 | 649.6 | +0.3 | 652.8 | +0.8 | 649.4 | +0.3 |
| 0.10 | 650.7 | 653.9 | +0.5 | 656.5 | +0.9 | 655.2 | +0.7 |
| 0.20 | 666.1 | 659.5 | −1.0 | 661.2 | −0.7 | 662.9 | −0.5 |
| 0.30 | 670.4 | 664.1 | −0.9 | 665.5 | −0.7 | 669.8 | −0.09 |

Table 3
Experimental and theoretical values of the breakthrough times for various values of $C_{d,out}/C_{d,in}$ when $C_{d,in}=0.03$ kg/m$^3$

| $C_{d,out}/C_{d,in}$ | Breakthrough time (min) | | | | | | |
|---|---|---|---|---|---|---|---|
| | Experimental value | Case 1 | | Case 2 | | Case 3 | |
| | | Theoretical value | % diff. | Theoretical value | % diff. | Theoretical value | % diff. |
| 0.01 | 227.1 | 242.8 | +6.9 | 239.6 | +5.5 | 234.3 | +3.2 |
| 0.05 | 235.2 | 245.2 | +4.2 | 242.8 | +3.2 | 239.9 | +2.0 |
| 0.10 | 241.9 | 246.4 | +1.9 | 244.3 | +1.0 | 242.4 | +0.2 |
| 0.20 | 246.8 | 247.8 | +0.4 | 246.0 | −0.3 | 245.5 | −0.5 |
| 0.30 | 250.1 | 249.5 | −0.2 | 248.2 | −0.8 | 249.6 | −0.2 |

Table 4
Experimental and theoretical values of the breakthrough times for various values of $C_{d,out}/C_{d,in}$ when $C_{d,in}=0.05$ kg/m$^3$

| $C_{d,out}/C_{d,in}$ | Breakthrough time (min) | | | | | | |
|---|---|---|---|---|---|---|---|
| | Experimental value | Case 1 | | Case 2 | | Case 3 | |
| | | Theoretical value | % diff. | Theoretical value | % diff. | Theoretical value | % diff. |
| 0.01 | 138.7 | 147.1 | +6.0 | 148.4 | +7.0 | 145.9 | +5.2 |
| 0.05 | 146.4 | 149.2 | +1.9 | 150.1 | +2.5 | 149.3 | +2.0 |
| 0.10 | 149.7 | 150.1 | +0.3 | 150.9 | +0.8 | 150.1 | +0.3 |
| 0.20 | 152.3 | 151.0 | −0.8 | 151.8 | −0.3 | 151.5 | −0.5 |
| 0.30 | 154.0 | 152.4 | −1.0 | 152.8 | −0.8 | 153.2 | −0.5 |

experimental data at 1% and 5% breakthrough and using the estimated values of $D_p$ and $C_T$ of Case 3 improves the agreement at 1% and 5% breakthrough even more. The differences between the experimental breakthrough times and the breakthrough times predicted by the nonlinear model using the estimated value of $D_p$ of Case 1 for $C_{d,in}=0.05$ kg/m$^3$ in Table 4 are not as large as the corresponding differences for $C_{d,in}=0.03$ kg/m$^3$ in Table 3. Furthermore, using the estimated parameter values of Cases 2 and 3 does not improve the agreement between the model and the experimental data at 1% and 5% breakthrough for $C_{d,in}=0.05$ kg/m$^3$. The differences between the predictions of the nonlinear model and the experimental data are very small for 10%, 20% and 30% breakthrough for all three cases for both $C_{d,in}=0.03$ kg/m$^3$ and $C_{d,in}=0.05$ kg/m$^3$. Taken as a whole, the results in Tables 2–4 indicate that the dynamic nonlinear adsorption model for purely diffusive particles with a monodisperse porous structure can represent the experimental data very well, especially if one considers the possible experimental uncertainties.

The values of the effective pore diffusion coefficient, $D_p$, that were estimated for all cases are presented in Table 5. For all three values of $C_{d,in}$, the values of $D_p$ that were estimated for the dynamic nonlinear model in Cases 1–3 are less than the value of the free molecular diffusivity of BSA ($5.9\times10^{-11}$ m$^2$/s [25]), indicating that they are physically realistic. For Case 1, in which the experimental points are evenly weighted, the value of $D_p$ decreases when the value of $C_{d,in}$ is increased. When the experimental points on the lower half of the breakthrough curve are more heavily weighted as for Case 2, the value of $D_p$ for $C_{d,in}=0.03$ kg/m$^3$ decreases 20%, while the values of $D_p$ for $C_{d,in}=0.01$ and 0.05 kg/m$^3$ each increase 14%. When $C_T$ is used as an additional parameter as for Case 3, the values of $D_p$ decrease by 30–40%, although the estimated values of $C_T$ are less than 2.5% different than the value of $C_T$ estimated from the equilibrium data. Even small changes in the value of $C_T$ can affect the value of $D_p$ greatly, indicating the importance of accurately measuring the value of $C_T$ and the large effect of the value of $C_T$ on the performance of adsorption systems, as found and shown in earlier work [13].

The value of $D_p$ that was estimated by fitting the

Table 5
Estimated values of the effective pore diffusion coefficient, $D_p$

| $C_{d,in}$ (kg/m$^3$) | $D_p$ (m$^2$/s) | | | | | |
|---|---|---|---|---|---|---|
| | Case 1 | Case 2 | Case 3[a] | Case 4 | Case 5 | Case 6[b] |
| 0.01 | $4.11\times10^{-11}$ | $4.69\times10^{-11}$ | $2.95\times10^{-11}$ | $4.11\times10^{-11}$ | $4.11\times10^{-11}$ | $2.77\times10^{-9}$ |
| 0.03 | $2.93\times10^{-11}$ | $2.33\times10^{-11}$ | $1.34\times10^{-11}$ | $2.94\times10^{-11}$ | $2.93\times10^{-11}$ | – |
| 0.05 | $2.00\times10^{-11}$ | $2.27\times10^{-11}$ | $1.57\times10^{-11}$ | $2.00\times10^{-11}$ | $2.00\times10^{-11}$ | – |

[a] The values of $C_T$ that were estimated in Case 3 are $C_T=51.56$ kg/m$^3$ for $C_{d,in}=0.01$ kg/m$^3$, $C_T=52.08$ kg/m$^3$ for $C_{d,in}=0.03$ kg/m$^3$ and $C_T=51.56$ kg/m$^3$ for $C_{d,in}=0.05$ kg/m$^3$.
[b] The value of $H$ that was estimated in Case 6 is $H=4216.5$ for $C_{d,in}=0.01$ kg/m$^3$.

dynamic nonlinear adsorption model for purely diffusive adsorbent particles to the experimental breakthrough curves was found to decrease as the concentration of the adsorbate increased. This result is qualitatively consistent with the prediction of a model for restricted diffusion in porous adsorbents [26]. It would be of interest to fit the restricted diffusion model [26] to the dynamic experimental data of this work to determine the values of the parameters of the restricted diffusion model that could provide appropriate quantitative agreement between the predictions of the dynamic nonlinear adsorption model that uses the restricted diffusion model to describe the evolution of the effective pore diffusion coefficient, $D_p$, and the experimental breakthrough data.

Heeter and Liapis [21] have presented a method for estimating the potential importance of intraparticle convection in an adsorption system, if, hypothetically, it was assumed that there could be intraparticle fluid flow in the porous adsorbent particles of a chromatographic system of interest. Using the procedure of [21], the maximum value of $F$ for the adsorption system of this work was estimated to be between $F=1.6\times10^{-4}$ and $F=2.7\times10^{-4}$. The dynamic nonlinear adsorption model for perfusive adsorbent particles with a monodisperse porous structure was fitted to the experimental breakthrough curves for $C_{d,in}=0.01$, 0.03 and 0.05 kg/m$^3$ under two conditions. For Case 4, the value of $F=1.6\times10^{-4}$ was used, the Langmuir isotherm parameter values that were estimated from the equilibrium experimental data were used, and the value of $D_p$ that gave the best fit when the experimental points were evenly weighted was estimated. For Case 5, the value of $F=2.7\times10^{-4}$ was used, the Langmuir isotherm parameter values that were estimated from the equilibrium experimental data were used, and the value of $D_p$ that gave the best fit when the experimental points were evenly weighted was estimated.

The values of $D_p$ that were estimated for Cases 4 and 5, listed in Table 5, are nearly identical (less than 0.4% difference) to the values of $D_p$ that were estimated for Case 1 for $C_{d,in}=0.01$, 0.03 and 0.05 kg/m$^3$. Furthermore, the breakthrough curves predicted by the nonlinear adsorption model for perfusive particles using the parameter values of Cases 4 and 5 are indistinguishable from the breakthrough curves predicted by the nonlinear model for purely diffusive particles using the parameter values of Case 1, shown in Fig. 2. The maximum value of the intraparticle Peclet number, $Pe_{intra}$, for Cases 4 and 5 is in the range where earlier work [9,10] has shown that intraparticle fluid flow has an insignificant effect on the mass transfer of adsorbate in porous adsorbent particles. Therefore, the above analysis and the results in Figs. 2–4 and Tables 2–5 (Cases 1–5) indicate that it is appropriate to model Source 15Q anion-exchange particles as purely diffusive particles.

The dynamic linear adsorption model for purely diffusive adsorbent particles with a monodisperse porous structure was fitted to the experimental breakthrough curve for $C_{d,in}=0.01$ kg/m$^3$ and this is represented as Case 6 in this work. For Case 6, the values of $D_p$ and $H$ that gave the best fit in the Laplace transform domain when the experimental points were evenly weighted were estimated and are presented in Table 5. Fig. 5 compares the experimental breakthrough curve for $C_{d,in}=0.01$ kg/m$^3$ with the prediction of the dynamic linear model using the estimated parameter values of Case 6. The agreement between the dynamic linear model and the experimental data for $C_{d,in}=0.01$ kg/m$^3$ is as good as that for the dynamic nonlinear model. The value of

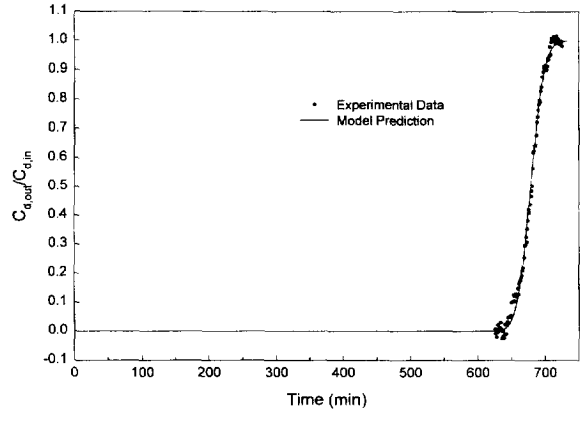


Fig. 5. Comparison of the experimental breakthrough curve for $C_{d,in}=0.01$ kg/m$^3$ with the predictions of the dynamic linear adsorption model for purely diffusive adsorbent particles with a monodisperse porous structure using the best estimate of $D_p$ when the experimental points are evenly weighted and $H$ is used as an adjustable parameter. $D_p=2.77\times10^{-9}$ m$^2$/s, $H=4216.5$.

$H$ that was estimated by fitting the dynamic data ($H=4216.5$) was very nearly the same as the value of $H=4210$ that would be obtained from Eq. (14) if it were assumed that the equilibrium data for $C_{d,in}=0.01$ kg/m$^3$ was located on a linear isotherm. However, the value of $D_p$ estimated for the dynamic linear model, listed in Table 5, is nearly two orders of magnitude larger than the free molecular diffusivity of BSA, and, when a physically reasonable value of $D_p$ (less than or equal to the free molecular diffusivity of BSA) is used, the breakthrough curve predicted by the dynamic linear model is much too dispersive to adequately represent the experimental breakthrough data for $C_{d,in}=0.01$ kg/m$^3$, indicating that the dynamic linear adsorption model is not appropriate for the adsorption of BSA onto Source 15Q anion-exchange particles when $C_{d,in}=0.01$ kg/m$^3$. The procedure of fitting the dynamic linear adsorption model to experimental breakthrough data could serve as an effective means of determining whether the adsorption mechanism of a particular adsorption system is linear or nonlinear. If the value of $D_p$ that is estimated for the dynamic linear adsorption model is physically reasonable, then the dynamic linear adsorption model could be considered appropriate for the adsorption process in question. Moreover, since parameter estimation for the dynamic linear adsorption model can be done in the Laplace transform domain [16], the computational effort required to make this determination would be relatively small.

## 5. Conclusions and remarks

Experimental data from a column adsorption system involving the adsorption of BSA onto Source 15Q anion-exchange adsorbent particles were presented for several values of the column inlet adsorbate concentration, $C_{d,in}$. The equilibrium experimental data for this system were well represented by the Langmuir equilibrium isotherm model in the adsorbate concentration range studied.

The dynamic nonlinear adsorption model for purely diffusive adsorbent particles with a monodisperse porous structure was fitted to the experimental breakthrough curves for three different values of $C_{d,in}$ and the overall agreement between this model and the experimental data was excellent, although the model tended to predict the earliest breakthrough times to be slightly later than the experimental data. When the experimental points on the lower half of the breakthrough curve were weighted more heavily than those on the upper half of the breakthrough curve, there was a modest improvement in the prediction of the earliest breakthrough times. The observed variation in the value of the effective pore diffusion coefficient, $D_p$, that was estimated for the dynamic nonlinear model with changes in the value of $C_{d,in}$ is consistent with the predictions of a model for restricted diffusion in porous adsorbents [26]. Future work could be directed toward reanalysing the experimental data of this work using the restricted diffusion model.

A previously presented [21] method for estimating the potential importance of intraparticle convection in an adsorption system was used to obtain estimates of the maximum value of the parameter $F$, which characterizes the mechanism of intraparticle convection, if it is hypothetically assumed that there could be intraparticle fluid flow in the particles; the estimated values of $F$ were very small. The values of $D_p$ that were estimated by fitting the dynamic nonlinear adsorption model for perfusive adsorbent particles with a monodisperse porous structure to the experimental breakthrough curves using the estimated maximum values of $F$ were nearly identical (less than 0.4% difference) to the values of $D_p$ that were estimated for the nonlinear adsorption model for purely diffusive particles and the breakthrough curves predicted by the model for perfusive particles were indistinguishable from the breakthrough curves predicted by the model for purely diffusive particles. The results of this work indicate that the dynamic nonlinear adsorption model for purely diffusive particles describes most appropriately the experimental breakthrough curves of the system studied in this work, and, therefore, the results show that it is appropriate to model Source 15Q anion-exchange particles as purely diffusive particles.

The dynamic linear adsorption model for purely diffusive adsorbent particles with a monodisperse porous structure was fitted to the experimental breakthrough curve for the smallest value of $C_{d,in}$ studied. While the agreement between the dynamic linear adsorption model and the experimental data

was as good as that for the dynamic nonlinear adsorption model, the value of the effective pore diffusion coefficient, $D_p$, that was estimated for the dynamic linear adsorption model is much larger than the free molecular diffusivity of BSA, indicating that the dynamic linear adsorption model is not appropriate for this adsorption system at this adsorbate concentration. The physical reasonableness of the estimated value of $D_p$ for the dynamic linear adsorption model could serve as a criterion for determining whether the adsorption mechanism of an adsorption system is linear or nonlinear.

## 6. Symbols

| | |
|---|---|
| $C_d$ | concentration of adsorbate in the flowing fluid stream of the column (kg/m$^3$ of bulk fluid) |
| $C_{d,in}$ | concentration of adsorbate at the column inlet (kg/m$^3$ of bulk fluid) |
| $C_{d,out}$ | concentration of adsorbate at the column outlet (kg/m$^3$ of bulk fluid) |
| $C_p$ | concentration of adsorbate in the fluid of the pores of the adsorbent particle (kg/m$^3$ of pore fluid) |
| $\bar{C}_p$ | average concentration of adsorbate in an adsorbent particle with a monodisperse porous structure given by Eq. (2) (kg/m$^3$ of adsorbent particle) |
| $C_s$ | concentration of adsorbate in the adsorbed phase of the adsorbent particle (kg/m$^3$ of adsorbent particle) |
| $C_s^*$ | equilibrium adsorbate concentration in the adsorbed phase of the adsorbent particle when the equilibrium adsorbate concentration in the pore fluid is equal to $C_{d,in}$ (kg/m$^3$ of adsorbent particle) |
| $C_T$ | maximum equilibrium concentration of adsorbate in the adsorbed phase of the adsorbent particle in the Langmuir isotherm model (kg/m$^3$ of adsorbent particle) |
| $d_p$ | diameter of adsorbent particle (m) |
| $D_p$ | effective pore diffusion coefficient of adsorbate (m$^2$/s) |
| $F$ | intraparticle convection parameter in Eqs. (12) and (13) (dimensionless) |
| $H$ | equilibrium adsorption constant for the linear isotherm model (dimensionless) |
| $K$ | equilibrium adsorption constant for the Langmuir isotherm model (m$^3$ of pore fluid/kg) |
| $L$ | column length (m) |
| $Pe_{intra}$ | intraparticle Peclet number (dimensionless) |
| $R$ | radial distance in adsorbent particle (m) |
| $R_p$ | radius of adsorbent particle (m) |
| $t$ | time (s) |
| $t_b$ | breakthrough time for which $C_{d,out} = C_{d,in}$ (s) |
| $v_{pR}$ | intraparticle velocity component along the $R$ direction (m/s) |
| $v_{p\theta}$ | intraparticle velocity component along the $\theta$ direction (m/s) |
| $\mathbf{v}_p$ | intraparticle velocity vector (m/s) |
| $V_f$ | column fluid superficial velocity (m/s) |
| $x$ | axial distance in column (m) |

Greek Letters

| | |
|---|---|
| $\varepsilon$ | void fraction of column |
| $\varepsilon_p$ | void fraction of adsorbent particles |
| $\theta$ | polar coordinate angle (radians) |

## Acknowledgments

The authors gratefully acknowledge partial support of this work by Monsanto and the donation of adsorption columns by Pharmacia Biotech AB. Professor A.I. Liapis gratefully acknowledges the support provided through the Humboldt Research Prize awarded to him in 1996 by the Alexander von Humboldt Foundation in Bonn, Germany.

## References

[1] B.H. Arve, A.I. Liapis, AIChE J. 33 (1987) 179.
[2] B.H. Arve, A.I. Liapis, Biotechnol. Bioeng. 31 (1988) 240.
[3] M.A. McCoy, A.I. Liapis, J. Chromatogr. 548 (1991) 25.
[4] B.H. Arve, A.I. Liapis, Biotechnol. Bioeng. 30 (1987) 638.
[5] B.H. Arve, A.I. Liapis, Biotechnol. Bioeng. 32 (1988) 616.

[6] A.I. Liapis, M.A. McCoy, J. Chromatogr. 599 (1992) 87.
[7] M.A. McCoy, A.I. Liapis, K.K. Unger, J. Chromatogr. 644 (1993) 1.
[8] A.I. Liapis, M.A. McCoy, J. Chromatogr. A 660 (1994) 85.
[9] A.I. Liapis, Y. Xu, O.K. Crosser, A. Tongta, J. Chromatogr. A 702 (1995) 45.
[10] G.A. Heeter, A.I. Liapis, J. Chromatogr. A 711 (1995) 3.
[11] Y. Xu, A.I. Liapis, J. Chromatogr. A 724 (1995) 13.
[12] G.A. Heeter, A.I. Liapis, J. Chromatogr. A 734 (1996) 105.
[13] G.A. Heeter, A.I. Liapis, J. Chromatogr. A 743 (1996) 3.
[14] A. Tongta, A.I. Liapis, D.J. Siehr, J. Chromatogr. A 686 (1994) 21.
[15] A.I. Liapis, A. Tongta, O.K. Crosser, Math. Model. Sci. Comput. 5 (1995) 1.
[16] G.A. Heeter, A.I. Liapis, J. Chromatogr. A 760 (1997) 55.
[17] G.A. Heeter, Ph.D. Dissertation, Department of Chemical Engineering, University of Missouri-Rolla, Rolla, MO, 1997.
[18] M.A. McCoy, A.I. Liapis, J. Chromatogr. 548 (1991) 25.
[19] F.H. Arnold, H.W. Blanch, C.R. Wilke, Chem. Eng. J. 30 (1985) B25.
[20] G. Neale, N. Epstein, W. Nader, Chem. Eng. Sci. 28 (1973) 1865.
[21] G.A. Heeter, A.I. Liapis, J. Chromatogr. A 761 (1997) 35.
[22] Y. Xu, Ph.D. Dissertation, Department of Chemical Engineering, University of Missouri-Rolla, Rolla, MO, 1995.
[23] D.M. Ruthven, Principles of Adsorption and Adsorption Processes, John Wiley and Sons, New York, 1984, p. 271.
[24] Pharmacia Biotech AB, personal communication.
[25] H.A. Sober (Ed.), Handbook of Biochemistry: Selected Data for Molecular Biology, The Chemical Rubber Co., Cleveland, OH, 1968.
[26] J.H. Petropoulos, A.I. Liapis, N.P. Kolliopoulos, J.K. Petrou, N.K. Kanellopoulos, Bioseparation 1 (1990) 69.